https://doi.org/10.1007/s00586-019-06225-5

# Biomechanics of sacropelvic fixation: a comprehensive finite element comparison of three techniques

Fabio Galbusera[1], Gloria Casaroli[1], Ruchi Chande[2], Derek Lindsey[2], Tomaso Villa[3], Scott Yerby[2], Ali Mesiwala[4], Matteo Panico[1,3], Enrico Gallazzi[1], Marco Brayda-Bruno[1]

[1] Laboratory of Biological Structures Mechanics, IRCCS Istituto Ortopedico Galeazzi, via Galeazzi 4, 20161 Milan, Italy

[2] SI-BONE, Inc, San Jose, CA, USA

[3] Department of Chemistry, Materials and Chemical Engineering "Giulio Natta", Politecnico Di Milano, Milan, Italy

[4] Southern California Center for Neuroscience and Spine, Pomona, CA, USA

Corresponding author

Fabio Galbusera - fabio.galbusera@grupposandonato.it

Keywords Pelvic fixation, Alar-iliac screws, Iliac screws, Screw loosening, Micromotion, Pseudoarthrosis

**Abstract**

**Purpose** Sacropelvic fixation is frequently used in combination with thoracolumbar instrumentation for complex deformity correction and is commonly associated with pseudoarthrosis, implant failure and loosening. This study compared pedicle screw fixation (PED) with three different sacropelvic fixation techniques, namely iliac screws (IL), S2 alar-iliac screws (S2AI) and laterally placed triangular titanium implants (SI), all in combination with lumbosacral instrumentation, accounting for implant micromotion.

**Methods** Existing finite element models of pelvis-L5 of three patients including lumbopelvic instrumentation were utilized. Moments of 7.5 Nm in the three directions combined with a 500 N compressive load were simulated. Measured metrics included flexibility, instrumentation stresses and bone–implant interface loads.

**Results** Fixation effectively reduced the sacroiliac flexibility. Compared to PED, IL and S2AI induced a reduction in peak stresses in the S1 pedicle screws. Rod stresses were mostly unaffected by S2AI and SI, but IL demonstrated a stress increase. In comparison with a previous work depicting full osteointegration, SI was found to have similar instrumentation stresses as those due to PED.

**Conclusions** Fixation with triangular implants did not result in stress increase on the lumbosacral instrumentation, likely due to the lack of connection with the posterior rods. IL and S2AI had a mild protective effect on S1 pedicle screws in terms of stresses and bone–implant loads. IL resulted in an increase in the rod stresses. A comparison between this study and previous work incorporating full osteointegration demonstrates how these results may be applied clinically to better understand the effects of different treatments on patient outcomes.

## Introduction

Achieving a solid and stable fixation of the lumbosacral junction during the surgical treatment of adult spinal deformities is a notoriously challenging task resulting in a high risk of postoperative complications such as pseudoarthrosis, implant failure and loosening [1–3]. A number of factors such as the low mechanical strength of bone tissue in the sacrum, the large loads acting in the lumbar spine and pelvis that result in a high risk of pullout, and loosening of the instrumentation, as well as the technical complexity of some of the most effective surgical techniques, contribute to such common unsatisfactory clinical outcomes [1, 4]. To that end, sacropelvic fixation, such as iliac and S2AI screws, has been added to the inferior end of the long construct to mitigate the aforementioned issues. Such methods of supplementation have been studied and compared [5–10], but loosening still persists [4].

Several biomechanical studies based on in vitro testing of cadaveric specimens investigated the differences between the various surgical options for lumbosacral and lumbopelvic fixation in terms of flexibility [11–14], and in some cases, surface strains in the instrumentation by means of strain gauges [15–18]. Although the scientific relevance of these studies is indisputable, the inherent limitations of the available technologies prevent their use in the investigation of several relevant quantities. Such quantities include full-field local stresses and strains in the instrumentation or interface forces between the implants and the adjacent tissues, which may indicate the risk of loosening and pullout. In fact, the accurate assessment of instrumentation loosening remains out of the scope of most biomechanical in vitro studies.

From a theoretical point of view, finite element modeling offers a powerful alternative to in vitro experiments for such investigations since it allows estimating the value of any mechanical quantity in the model [19]. However, most models involve several simplifications and assumptions in order to limit their technical complexity and computational cost, thus practically precluding their use for the prediction of quantities which are not measurable in vitro as well. One of these common simplifications concerns the issue of the interaction between implants and bone. Most studies about spinal implants, including our previous paper about sacropelvic fixation [20], assumed a rigid kinematic coupling not allowing for any relative motion, implemented by means of kinematic constraints, bonded contacts and

connectors or embedded elements [21–24]. Such methods are meant to replicate the long-term condition after a successful osteointegration and have been used to investigate implant stresses with the associated risk of mechanical failure [25], long-term kinematics [26, 27] as well as stresses in the adjacent biological tissues [28, 29].

However, assuming no relative motion at the bone–implant interface may not well represent the immediate postoperative stage before bone ingrowth takes place nor the clinical cases in which a successful osteointegration is not achieved. As mentioned above, the latter outcome is relatively frequent after lumbosacral and sacropelvic fixations, which are associated with high occurrences of implant loosening and pseudoarthrosis [1, 2, 30–32]. However, despite the clinical relevance of the topic, no existing finite element model of sacropelvic fixation accounts for a lack of osteointegration of the implants.

The aim of the present study was to investigate the biomechanics of sacropelvic fixation by means of three different techniques replicating a lack of perfect osteointegration by introducing a mechanically realistic model of the implant–bone interface. To this aim, we simulated the micromotion of instrumentation implanted in the pelvis by means of phenomenological models calibrated against experimental tests conducted on synthetic bone blocks. Measured metrics included flexibility, stresses on the instrumentation and axial loads at the bone–implant interface, assumed as indicators of the risk of loosening.

## Materials and methods

### Finite element models

Three finite element models of the pelvis and lower lumbar spine developed in a previous study [20] were used as a basis for the investigation of the effects of micromotion at the implant–bone interface. The models represented the anatomy of three female adult subjects acquired by means of CT scans and reconstructed with in-house software; written informed consent for the use of the imaging data for research purposes was previously obtained. A detailed description of meshes, element types, material properties, as well as flexibility validation, is reported elsewhere [20].

Similar to the previous studies, the three spinopelvic models were used to simulate four different fixation configurations: (1) posterior rods in lumbar spine and pedicle screws in S1 (PED); (2) lumbosacral pedicle screw fixation as in PED in combination with bilateral iliac screws (IL); (3) lumbosacral fixation in combination with bilateral alar-iliac screws in S2 (S2AI); (4) lumbosacral fixation in combination with bilateral instrumentation of the SI joint with three triangular titanium implants (iFuse Implant System, SI-Bone, Inc., Santa Clara, CA, USA) not connected to the posterior rods (SI) (Fig.

1). In all models, the posterior rods had a diameter of 5.5 mm; pedicle screws had a length of 40 mm and diameter of 6.5 mm; alar-iliac screws had a length of 65 mm and diameter of 6.5 mm; iliac screws had a length of 75 mm and diameter of 7.5 mm; triangular implants had a diameter of 7 mm and length of 65 mm. All implants were modeled as having the material properties of titanium (elastic modulus of 110 GPa and Poisson's ratio of 0.3). Posterior rods were modeled as beam elements with circular section.

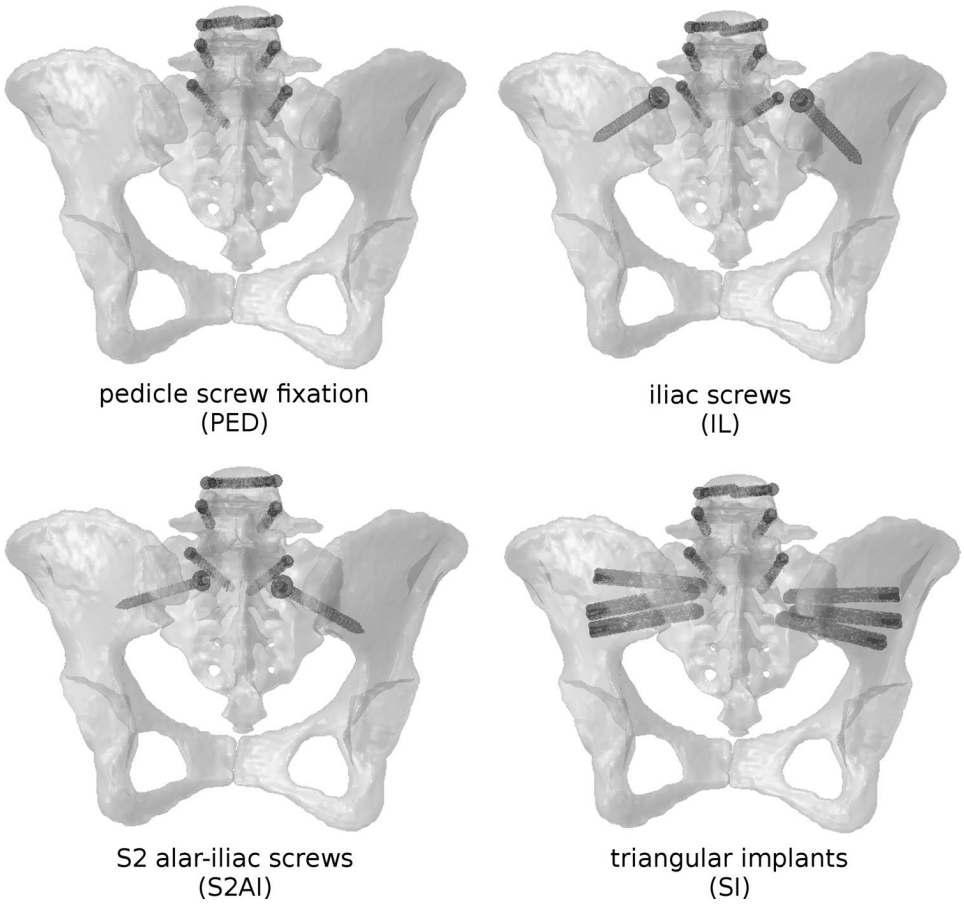


*Fig. 1 Renderings of the four implanted configurations investigated: pedicle screw fixation to S1 (PED), lumbosacral fixation with pedicle screws supplemented by iliac screws (IL) and by S2 alar-iliac screws (S2AI), lumbosacral posterior fixation supplemented with sacroiliac fixation with laterally placed triangular implants (rods not shown)*

**Implant–bone interaction**

Regarding the lumbar instrumentation, the interaction between pedicle screws and bone was modeled by means of embedded elements, which consist of a kinematic coupling between the external nodes of the screws and the adjacent nodes in the bone tissue, thus neglecting relative displacements at the interface [22].

In the sacrum and ilium [31, 32], we employed a modeling approach to simulate the interaction between bone and S1 pedicle screws, iliac screws, alar-iliac screws as well as triangular implants, which we named "partially embedded model" (P-EM) in contrast with the fully embedded elements (F-EM) which have been employed in our previous study [20]. This phenomenological modeling strategy was based on two sets of linear springs; the first set connected the nodes on the external surfaces of the implants with the closest nodes in the bone volumes, whereas the second one connected the nodes of the bone tissue in the proximity of the implant surface with the closest node of the beam elements representing the relevant rod (Fig. 2). Because the triangular implants are not connected to the posterior rods, only the first set of springs was implemented.

The stiffness of the springs was calibrated in order to match the mechanical response of the bone–implant construct as measured in experimental tests. To this purpose, pull-out and torsional tests were conducted using pedicle screws implanted in blocks of synthetic bone (Fig. 2). A finite element model of the block-screw construct having the same geometry and material properties was built and used to determine the optimal values of the stiffness of the two groups of springs defined as those which minimized the error with respect to the experimental results. Those values were, therefore, employed for modeling the bone–implant interactions in the pelvis in all the subsequent analyses.

**Simulations and outputs**

All the anatomical models were used to simulate pure moments of 7.5 Nm in flexion, extension, lateral bending and axial rotation in both directions in combination with a compressive follower load of 500 N [33]. Single-leg stance [34] was simulated by constraining all nodes belonging to each cotyloid cavity, one at a time; therefore, 12 simulations for each model were run resulting in a total of 36 simulations. For the sake of validation, comparison of the flexibility of the implanted configurations with available in vitro data [12, 34] was performed.

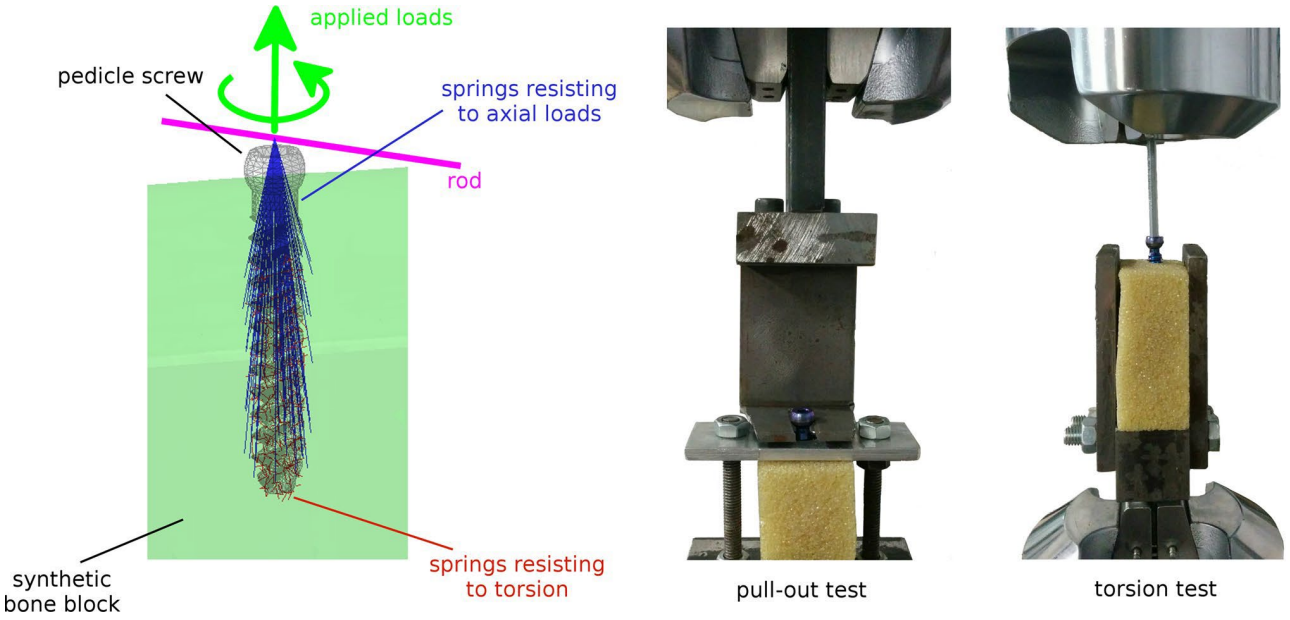


*Fig. 2 (left) Schematic representation of the finite element approach used to model micromotions between the implants and the surrounding bone tissue, here replaced by a synthetic bone block used to calibrate the stiffness of the springs. Two sets of linear springs are defined: the first set (in red) connects the nodes on the external surfaces of the implants with the closest nodes in the bone volumes, whereas the second one (in blue) connected the nodes of the bone tissue in the proximity of the implant surface with the closest node of the beam elements representing the rod. Custom fixtures used for the pull-out test (center) and for the torsion test (right)*

The outputs of the simulations were: (1) the range of motion of the SIJ for the various fixation configurations, as well as the percent change in motion with respect to the intact value; (2) the maximal von Mises stresses in the S1 pedicle screws; (3) the maximal stresses in the posterior rods between the pedicle screws in L5 and S1 (i.e., lumbosacral junction); (4) the longitudinal component, i.e., the one along the direction of the implant, of the force at the interface between the S1 pedicle screws and the adjacent bone tissue (i.e., the pull-out or push-in force); (5) the axial component of the interface forces for the sacropelvic fixation implants, i.e., iliac and S2AI screws as well as the triangular implants, which we assume to be associated with the risk of loosening. Bone–implant interface forces were calculated as the *resultant* of the forces in the two sets of spring elements projected along the direction of the implant. Fixation was observed on both the ipsilateral and contralateral sides relative to the boundary conditions, and ipsilateral (and thereby the contralateral) represented either the right or left side (Fig. 3).

Finally, a comparison of the modeling technique used in the current study, specifically the use of partially embedded elements, with the fully embedded element technique described in [20] was made by examining the effects on S1 pedicle screw stress and rod stress.

## Results

### Validation and flexibility

The comparison with existing in vitro flexibility data about pedicle screw fixation, sacropelvic fixation with iliac and S2AI screws [12] as well as with the triangular titanium implants [34] showed a generally good agreement with the largest deviations found in axial rotation for PED and IL (Fig. 4). Generally, sacropelvic fixation resulted in a decrease in range of motion in comparison with PED and the intact conditions (Fig. 5).

Pedicle screw fixation of the lumbosacral joint (PED) resulted in an increase in ROM from the intact condition (Table 1). Further, sacropelvic fixation induced a decrease in motion at the sacroiliac joint with fixation via SI demonstrating the most reduction relative to intact (57%, 53% and 73% in flexion/extension, lateral bending and axial rotation, respectively) and PED (approximately 80% in flexion/extension and lateral bending, and 73% in axial rotation). S2AI and IL resulted in a similar biomechanical response of the SIJ, which was markedly stiffer than PED only in flexion/ extension.

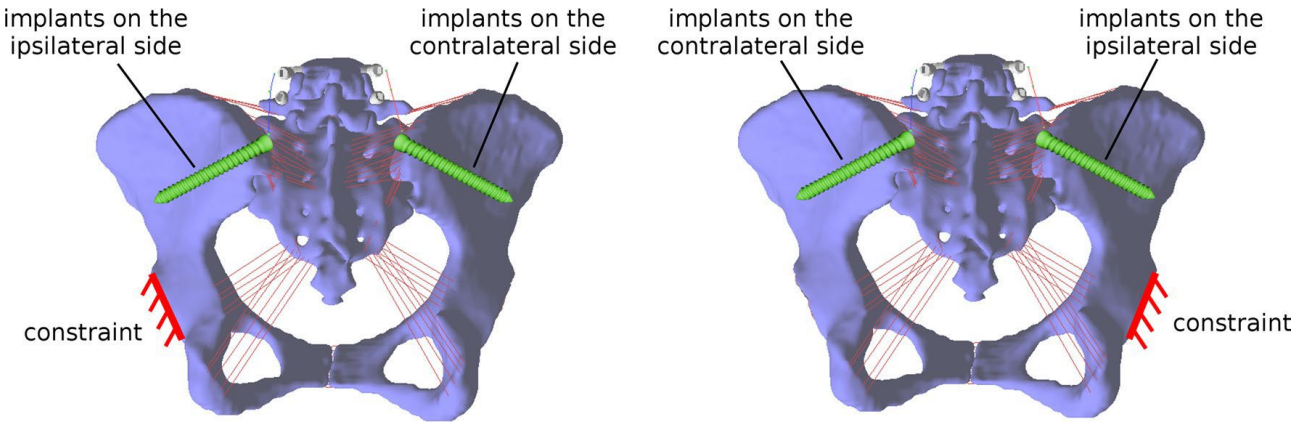


*Fig. 3 Conventional naming scheme for the implants used in the data analysis. The ipsilateral group of implants consists of those on the left side for the simulations in which the left cotyloid cavity was constrained (left), as well as of those on the right side for the simulations in which the boundary condition was applied to the right* cotyloid *cavity (right). Implants on the opposite side were named as contralateral*

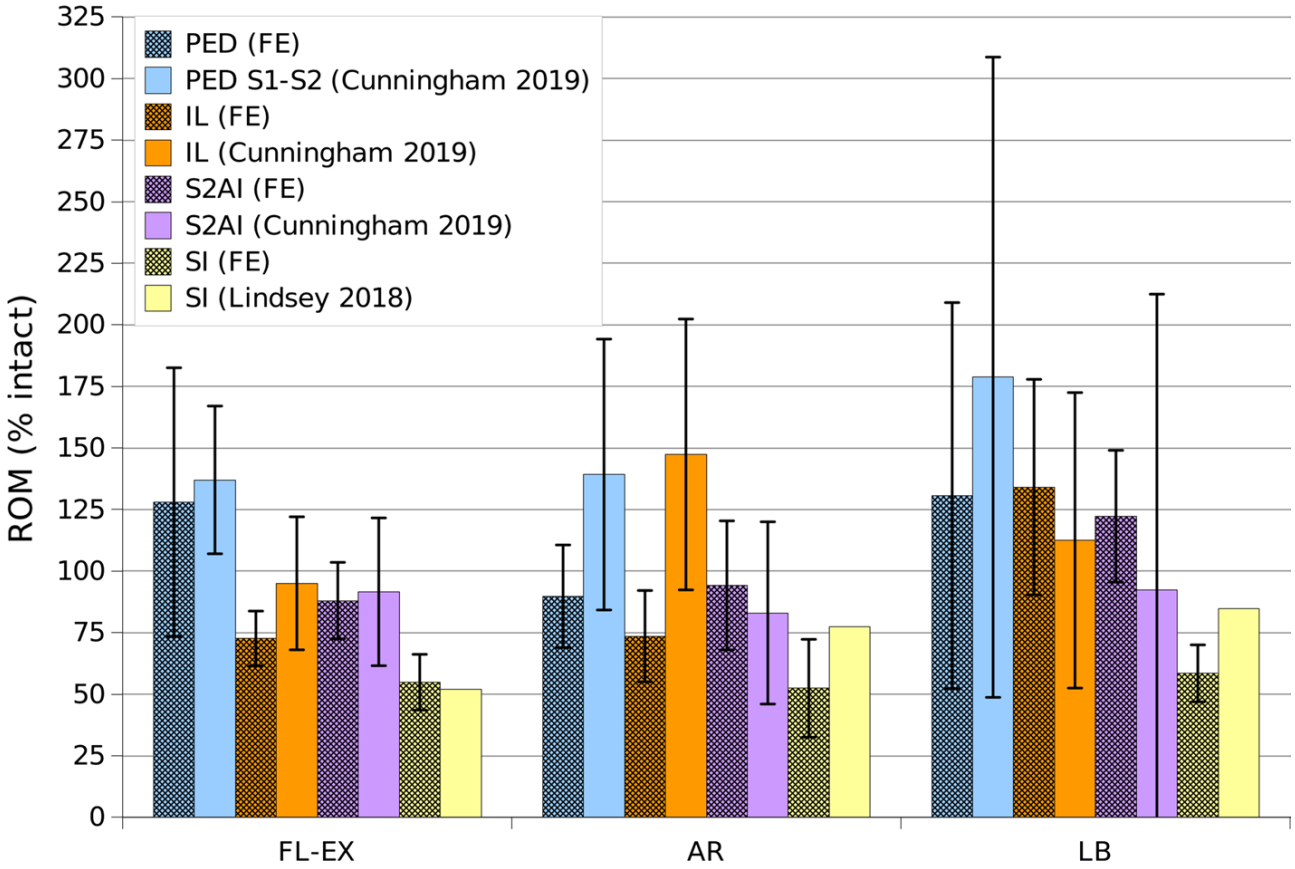


*Fig. 4 Relative ranges of motion of the SIJ (with respect to the intact condition) predicted for the four implanted configurations (PED, IL, S2AI and SI), as compared with relevant in vitro data available in the literature [12, 34]. For consistency with the in vitro data, finite element results are shown as average values and standard deviations among* the *six SIJs of the three patients. "FL-EXT": total range of motion in flexion–extension; "AR": total range of motion in left–right axial rotation; "LB": total range of motion in left–right lateral bending. "*" indicates statistically significant differences between the numerical predictions for the various configurations*

**S1 pedicle screws**

The maximal von Mises stresses in the S1 pedicle screws on the ipsilateral side (i.e., the same side of the applied boundary condition at the acetabulum) were on the same order of magnitude as those on the contralateral side. Compared to PED, IL and S2AI each resulted in some reduction in the maximum stresses observed in the S1 pedicle screws, whereas fixation using SI resulted in stresses similar to those induced by PED (Fig. 6).

Regarding forces transmitted at the bone–implant interface along the S1 pedicle screw direction, the highest pullout values were observed during flexion (55 MPa) and contralateral lateral bending (66 MPa). Generally, forces due to SI tended to be similar to those due to PED alone, while IL resulted in similar or

increased forces along the S1 pedicle screw relative to PED. Finally, flexion and ipsilateral axial rotation generally resulted in more pull-out forces, rather than push-in, across all configurations.

**Posterior rods**

When lumbopelvic fixation was compared to lumbosacral fixation (PED) alone, IL generally tended to increase the stresses on the L5S1 rods in all motions, whereas stresses due to S2AI and SI were comparable to PED (Fig. 7). This was generally true whether the examined rod was on the ipsilateral or contralateral side relative to the boundary condition.

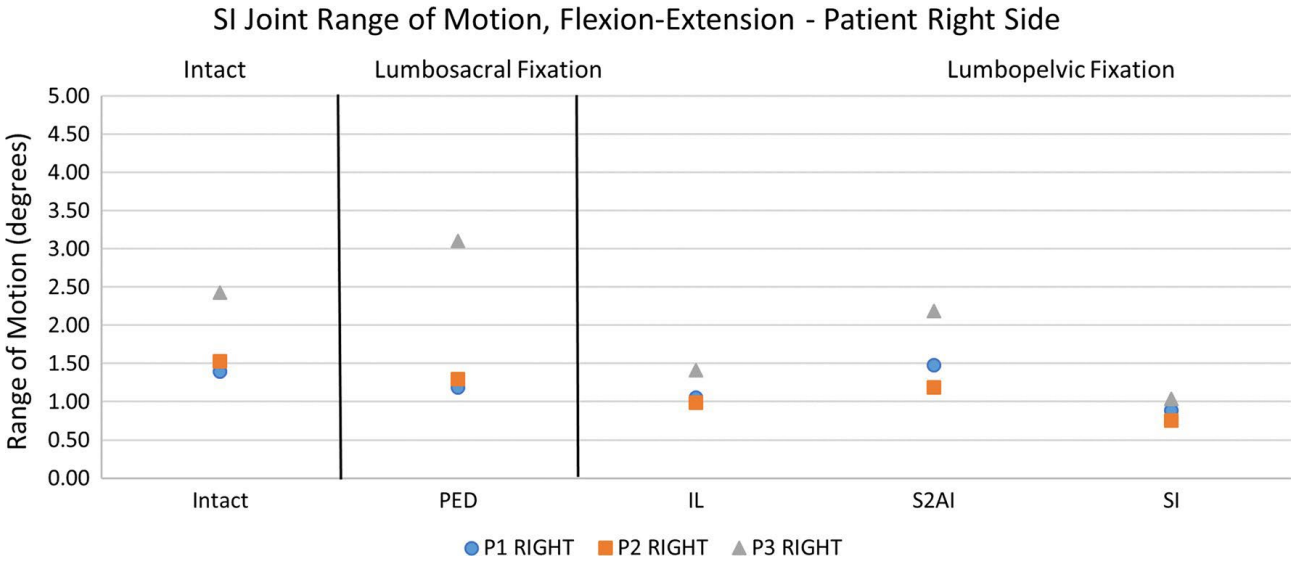


*Fig. 5 Range of motion in flexion–extension for the intact condition and four fixed configurations (PED, IL, S2AI, SI); data for three patient models*

**Axial forces at the interface between bone and sacropelvic fixation implants**

On the ipsilateral side of the boundary condition, pushin force values up to 145 N were predicted for the iliac screws. The highest pull-out forces (approximately 33 N for S2AI and 80 N for IL) on either ipsilateral or contralateral side, however, were less than the maximum push-in forces observed.

**Comparison between modeling techniques: fully embedded and partially embedded elements**

Stresses in S1 pedicle screws and rods predicted with P-EM and F-EM [20] were compared on the ipsilateral side of the boundary condition. S1 pedicle screw stresses generally decreased following the application of the partially embedded element technique for the PED and IL configurations, whereas the

direction of change for the S2AI configuration varied. Finally, SI demonstrated an increase in stresses (Table 2).

**Discussion**

In this paper, we modified existing finite element models of lumbosacral and sacropelvic fixation [20] by introducing elements accounting for the micromotion of the implants in the sacrum and pelvis, based on an experimental calibration conducted on synthetic bone blocks. By employing this numerical technique, we aimed at simulating a condition in which implant osteointegration did not take place, such as in the immediate postoperative stage or in the case of failed fusion. Notably, the current simulations reproduce the same condition of most in vitro tests in which the implantation is performed right before the test itself and no osteointegration exists.

In general terms, the results demonstrated that the techniques currently used for sacropelvic fixation are able to stabilize the SIJ and reduce its motion relative to the PED configuration. These findings closely confirmed the measurements published in a recent in vitro paper [12] in which pedicle screw fixation in the lumbosacral spine alone or supplemented by either iliac screw or S2 alar-iliac screw was tested in 21 human specimens. In line with previous studies, SIJ flexibilities of IL and S2AI constructs [12, 14] generally appeared similar to one another. The finite element ROM predictions for the SI configuration were also found to be consistent with published in vitro data [34, 35]. To our knowledge, in vitro studies comparing the SIJ flexibility after fixation with triangular implants against fixation via other techniques such as iliac or S2AI screws do not currently exist.

IL and S2AI reduced the stresses in S1 pedicle screws, whereas SI generally retained similar S1 pedicle screw stresses as the PED configuration. This finding demonstrates that the addition of sacropelvic implants will not worsen the stresses exhibited by S1 pedicle screws (in the case of SI) and may even offer some protection to the S1 pedicle screws in the case of IL and S2AI.

With regard to the posterior rods, IL tended to increase the stresses observed relative to PED, while similar results between PED, S2AI and SI were noted. This indicates that sacropelvic fixation does not offer any notable protection to the posterior rods and, in the case of IL, may have the undesired effect of worsening the stress profile. Rod stresses, however, were in all cases below the yield strength of titanium. In general, indeed, rod stresses were lower than those observed in the S1 pedicle screws. These findings confirmed those of our previous finite element models [20] as well as those of a published in vitro investigation conducted on 14 human specimens [15] and on 6 calf specimens [16]; however, in the latter one, rod strains were not measured.

In one in vitro study conducted on human specimens that involved interbody stabilization at L5-S1 [36], S2AI fixation was found to protect S1 pedicle screws. Additionally, it was found to protect posterior rods when pure moments in lateral bending and axial rotation were applied. In general, both previous data and current results suggest that S2AI fixation may have a limited protective effect on the lumbosacral instrumentation, whereas iliac screws may increase the risk of mechanical failure of the rods at the lumbosacral junction.

The finite element predictions about the bone–implant interaction loads suggest that IL maintains or increases forces relative to PED (depending on the motion), while S2AI and SI maintain or decrease pull-out forces relative to PED. The highest forces between the bone and implant were observed in lateral bending on the contralateral side. To our knowledge, there is no previous study investigating this issue from a biomechanical point of view; the present paper should, therefore, be considered as a first step in this direction, and further studies, including in vitro studies, are warranted.

*Table 1 Range of motion, percent change relative to intact (left) and PED (right) for flexion–extension*

| Change in ROM, Flexion–Extension—% relative to intact | | | | |
|---|---|---|---|---|
| | PED | IL | S2AI | SI |
| P1 RIGHT | − 15.34 | − 24.81 | 5.59 | − 36.27 |
| P2 RIGHT | − 15.08 | − 35.42 | − 22.13 | − 50.55 |
| P3 RIGHT | 28.00 | − 41.73 | − 9.69 | − 57.34 |
| P1 LEFT | 115.38 | − 31.68 | − 35.28 | − 57.46 |
| P2 LEFT | 43.89 | − 11.23 | − 14.08 | − 32.51 |
| P3 LEFT | 11.16 | − 19.40 | 3.65 | − 36.61 |
| Change in ROM, Flexion–Extension—% relative to PED | | | | |
| IL | | S2AI | SI | |
| − 11.19 | | 24.73 | − 24.72 | |
| − 23.95 | | − 8.30 | − 41.77 | |
| − 54.48 | | − 29.45 | − 66.67 | |
| − 68.28 | | − 69.95 | − 80.25 | |
| − 38.31 | | − 40.29 | − 53.10 | |
| − 27.49 | | − 6.76 | − 42.97 | |

Negative value = decrease

*P1* patient, *P2* patient 2, *P3* patient 3

*Table 2 Comparison of instrumentation stress between models with osteointegration (fully embedded elements [20]) and models with relative bone–implant motion (partially embedded elements, current study)*

| Screw on the constrained side of the model | | | | | | | | | | | | |
|---|---|---|---|---|---|---|---|---|---|---|---|---|
| | FL | | EX | | AR (IPSI) | | AR (CONTRA) | | LB (IPSI) | | LB (CONTRA) | |
| | F-EM | P-EM | F-EM | P-EM | F-EM | P-EM | F-EM | P-EM | F-EM | P-EM | F-EM | P-EM |
| PED | 213 (84–446) | 64 (59–165) | 346 (104–562) | 298 (258–451) | 236 (166–685) | 179 (104–282) | 149 (98–404) | 264 (241–359) | 239 (174–535) | 197 (186–318) | 337 (156–476) | 222 (215–249) |
| IL | 190 (134–419) | 89 (73–167) | 173 (102–475) | 85 (79–218) | 178 (110–315) | 105 (44–177) | 121 (55–500) | 109 (105–203) | 166 (84–350) | 71 (29–97) | 121 (77–410) | 143 (102–207) |
| S2AI | 95 (86–119) | 73 (60–88) | 80 (71–125) | 134 (111–146) | 119 (108–178) | 80 (58–101) | 68 (37–339) | 225 (207–231) | 109 (92–206) | 137 (112–160) | 120 (65–179) | 116 (99–178) |
| SI | 138 (99–335) | 84 (59–165) | 135 (80–182) | 298 (258–451) | 111 (61–171) | 179 (104–282) | 98 (74–157) | 264 (241–359) | 148 (99–236) | 197 (197–318) | 110 (64–247) | 249 (222–249) |
| S1 Pedicle screw stress (MPa), median (range) | | | | | | | | | | | | |
| Rod on the constrained side of the model | | | | | | | | | | | | |
| | FL | | EX | | AR (IPSI) | | AR (CONTRA) | | LB (IPSI) | | LB (CONTRA) | |
| | F-EM | P-EM | F-EM | P-EM | F-EM | P-EM | F-EM | P-EM | F-EM | P-EM | F-EM | P-EM |
| PED | 24 (14–52) | 16 (12–36) | 34 (10–52) | 35 (29–50) | 31 (17–60) | 38 (37–50) | 43 (23–76) | 41 (34–49) | 38 (10–68) | 45 (25–54) | 29 (19–64) | 25 (11–54) |
| IL | 67 (28–110) | 46 (43–105) | 53 (18–64) | 72 (60–102) | 74 (29–100) | 72 (58–86) | 74 (40–95) | 65 (54–128) | 72 (30–97) | 70 (54–81) | 47 (23–79) | 74 (41–123) |
| S2AI | 22 (13–40) | 27 (19–40) | 26 (10–50) | 30 (28–63) | 44 (18–89) | 43 (31–44) | 33 (23–75) | 37 (29–53) | 48 (24–68) | 39 (22–55) | 28 (15–45) | 48 (12–63) |
| SI | 16 (10–44) | 13 (10–24) | 20 (12–61) | 34 (28–48) | 30 (19–37) | 37 (27–38) | 38 (22–69) | 33 (30–46) | 30 (12–78) | 45 (27–52) | 29 (10–43) | 15 (10–30) |
| Rod stress (MPa), median (range) | | | | | | | | | | | | |

*F-EM* Fully Embedded Models [20]

*P-EM* Partially Embedded Models (current study)

As mentioned above, in a previous paper we investigated the same configurations assuming a perfect osteointegration of the implants in the pelvis, thus modeling a longterm postoperative condition in which a successful fusion is achieved [20]. As expected, stress values in fully osteointegrated implants were higher than those in the current models since the lack of relative motion implies higher load transfer. However, in terms of general trends, the current results confirmed those previously found: S2AI and IL were able to reduce the peak stress in S1 pedicle screws in both studies, and IL resulted in a marked increase in the rod stresses between L5 and S1. The most significant difference between the two studies concerns the stresses in the S1 pedicle screws for the SI configuration. When perfect osteointegration was assumed, S1 pedicle screw stresses were effectively reduced by the triangular implants, while the same could not be said when implant motion was allowed. This makes sense given the allowance of relative motion between the bone and implants in the current study coupled with the lateral trajectory of the triangular titanium implants, which have no direct connection to the posterior rods. Ultimately, the comparison between the two studies demonstrates how boundary conditions between hardware and bone may be represented and the differences imparted. These results have clinical applications as the two studies allow for a better understanding of treatment options and depict the different outcomes (i.e., fusion vs hardware loosening) that a patient may experience as a result of receiving a long construct with sacropelvic fixation.

Unlike in the large majority of available finite element studies, we decided not to model the anatomy of a single representative patient but to consider three representative patients. Though the computational time increased, modeling single-leg stance conditions on both sides of the body allowed us to investigate flexibility, stress and load values for all the six SIJs included in the models, which allowed us

to make a more comprehensive analysis. With our paper, we would like to encourage other authors to employ a similar approach in their own numerical studies. Specifically, we recommend creating several anatomical models when investigating a clinically relevant research question and performing simulations for all of them following the principles of the in silico clinical trials [37]. Various tools for threedimensional reconstruction and finite element preprocessing available nowadays, the scriptable nature of finite element solvers, as well as the availability of powerful free software that facilitates the development of application-specific preprocessing tools, effectively improved the accessibility of such an approach in comparison with that a few years ago. As a matter of fact, although we used the same values of material properties for the three patients and we modeled the same surgical techniques in a consistent way, the variability of the predictions revealed that using a single patient anatomy could limit the conclusions of the study.

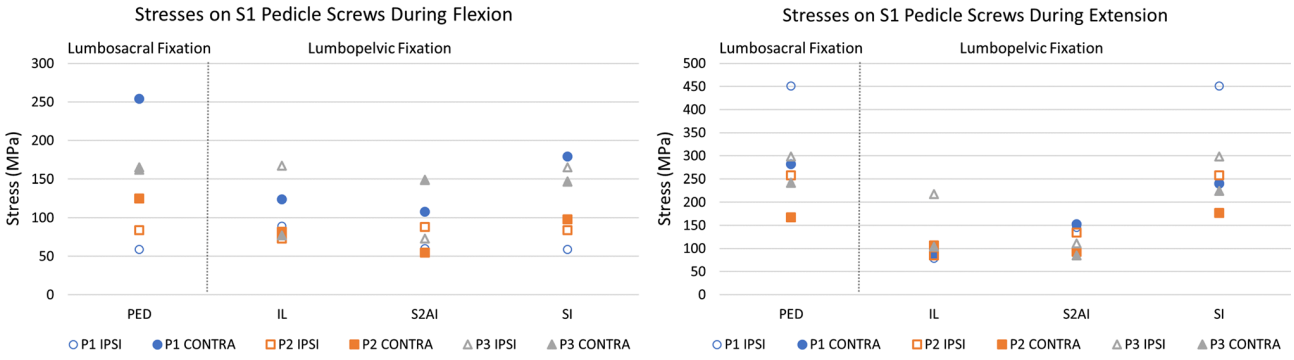


*Fig. 6 Stresses on S1 pedicle screws in flexion–extension for three patients due to thoracolumbar fixation alone (PED) and sacropelvic fixation (IL, S2AI, and SI)*

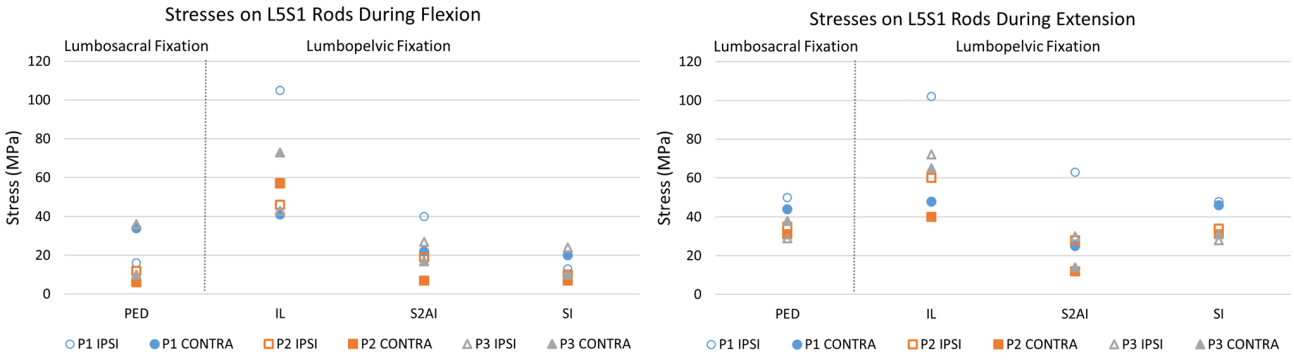


*Fig. 7 Stresses on L5S1 rods in flexion/extension for three patients due to thoracolumbar fixation alone (PED) and sacropelvic fixation (IL, S2AI and SI)*

**Limitations**

Although we employed sophisticated models with the aim of enhancing the accuracy of the predictions, this study still has some limitations. The approach used for the simulation of the bone–implant interface was phenomenological, i.e., it was aimed at replicating the global mechanical response of the construct, in terms of pull-out and torsional stiffness, which allowed for successful and accurate capture of the global response of the configurations without hindering the validity of the present results.

Loading and boundary conditions were based on those commonly used in in vitro and finite element studies [25, 33, 34, 38], which do not closely replicate the physiological ones but provide advantages in terms of comparability and reproducibility. To our knowledge, simplified loading conditions analogous to the present ones have been used to date in nearly all available finite models of spinal instrumentation. Indeed, comparisons with in vivo measurements obtained with telemeterized fixation implants revealed that simulating a follower compressive load in combination with pure moments allows obtaining realistic flexibilities, intradiscal pressures and strains in the instrumentation [39–41].

The spinopelvic models themselves included several simplifications especially in the L5-S1 segment, such as for the intervertebral disks and facet joints (described in detail in [20]). However, since the intact spinopelvic models proved to be valid in terms of flexibility, such simplifications can safely be assumed to have a negligible impact on the implant-related results here reported.

In order to investigate the risk of implant loosening, we assumed it to be associated with the force component along the main axis of the implant at the bone–implant interface. Although this assumption may be considered reasonable, it was not validated in a clinical setting; the interpretation of the bone–implant forces in terms of risk of loosening should therefore be considered only in qualitative terms. More sophisticated methods such as simulating the micromechanics of the bone–implant interaction [42] may in principle have allowed for more accurate results, but it would have required the introduction of further assumptions and extremely high computational resources.

**Conclusions**

In summary, the current simulations allowing for relative motion between the bone and implant interface revealed that all sacropelvic fixation techniques were able to reduce the flexibility of the SIJ in a comparable way with respect to the intact state and pedicle screw fixation. Sacroiliac fixation with triangular implants had no effect on the lumbosacral instrumentation due to the lack of connection with the posterior rods. Iliac screws and S2AI screws had a mild protective effect on the stresses in S1 pedicle screws, while iliac screws had a significant increase in the maximal rod stresses. Finally, comparisons between the current study and the previous study that modeled full osteointegration

demonstrated differences imparted as a result of the boundary conditions, and such results may be applied clinically to better understand treatment options and different patient outcomes.

**Acknowledgements**

Fabio Galbusera received research support from SI-BONE, Inc., to conduct this study.

**Author contribution**

GC, MP and FG developed the finite element models. FG developed the computer programs used for the pre-processing of the models. RC and DL supported and revised the development of the models. GC, RC, FG and DL prepared the draft of the manuscript. All authors critically evaluated and interpreted the results of the calculations, revised the manuscript and approved the submitted version.

**Funding**

The study has been funded by SI-BONE, Inc.

**References**

1. Esmende SM, Shah KN, Daniels AH (2018) Spinopelvic fixation. J Am Acad Orthop Surg 26(11):396–401. https: //doi.org/10.5435/JAAOS -D-15-00738

2. Kim YJ, Bridwell KH, Lenke LG et al (2006) Pseudarthrosis in long adult spinal deformity instrumentation and fusion to the sacrum: prevalence and risk factor analysis of 144 cases. Spine 31(20):2329–2336

3. Lee C, Chung SS, Choi SW et al (2010) Critical length of fusion requiring additional fixation to prevent nonunion of the lumbosacral junction. Spine 35(6):E206–E211

4. Kebaish KM (2010) Sacropelvic fixation: techniques and complications. Spine 35(25):2245–2251

5. Mazur MD, Ravindra VM, Schmidt MH et al (2015) Unplanned reoperation after lumbopelvic fixation with S-2 alar-iliac screws or iliac bolts. J Neurosurg Spine 23(1):67–76

6. Guler UO, Cetin E, Yaman O et al (2015) Sacropelvic fixation in adult spinal deformity (ASD); a very high rate of mechanical failure. Eur Spine J 24(5):1085–1091

7. Ilyas H, Place H, Puryear A (2015) A comparison of early clinical and radiographic complications of iliac screw fixation versus S2 alar iliac (S2AI) fixation in the adult and pediatric populations. J Spinal Disord Tech 28(4):E199–E205

8. Ishida W, Elder BD, Holmes C et al (2017) Comparison between S2-alar-iliac screw fixation and iliac screw fixation in adult deformity surgery: reoperation rates and spinopelvic parameters. Global Spine J 7(7):672–680

9. Elder BD, Ishida W, Lo SL et al (2017) Use of S2-alar-iliac screws associated with less complications than iliac screws in adult lumbosacropelvic fixation. Spine 42(3):E142–E149

10. Sohn S, Park TH, Chung CK et al (2018) Biomechanical characterization of three iliac screw fixation techniques: a finite element study. J Clin Neurosci 52:109–114

11. Burns CB, Dua K, Trasolini NA et al (2016) Biomechanical comparison of spinopelvic fixation constructs: iliac screw versus S2-alar-iliac screw. Spine Deform 4(1):10–15

12. Cunningham BW, Sponseller PD, Murgatroyd AA et al (2019) A comprehensive biomechanical analysis of sacral alar iliac fixation: an in vitro human cadaveric model. J Neurosurg Spine 30(3):367–375

13. Volkheimer D, Reichel H, Wilke H et al (2017) Is pelvic fixation the only option to provide additional stability to the sacral anchorage in long lumbar instrumentation? A comparative biomechanical study of new techniques. Clin Biomech 43:34–39

14. Hoernschemeyer DG, Pashuck TD, Pfeiffer FM (2017) Analysis of the s2 alar-iliac screw as compared with the traditional iliac screw: does it increase stability with sacroiliac fixation of the spine? Spine J 17(6):875–879

15. Hlubek RJ, Godzik J, Newcomb AGUS et al (2019) Iliac screws may not be necessary in long-segment constructs with L5–S1 anterior lumbar interbody fusion: cadaveric study of stability and instrumentation strain. Spine J. 19(5):942–950

16. Lebwohl NH, Cunningham BW, Dmitriev A et al (2002) Biomechanical comparison of lumbosacral fixation techniques in a calf spine model. Spine 27(21):2312–2320

17. Fleischer GD, Kim YJ, Ferrara LA et al (2012) Biomechanical analysis of sacral screw strain and range of motion in long posterior spinal fixation constructs: effects of lumbosacral fixation strategies in reducing sacral screw strains. Spine 37(3):E163–E169

18. Kleck CJ, Illing D, Lindley EM et al (2017) Strain in posterior instrumentation resulted by different combinations of posterior and anterior devices for long spine fusion constructs. Spine Deform 5(1):27–36

19. Galbusera F, Niemeyer F (2018) Mathematical and finite element modeling. Galbusera F. Elsevier, Amsterdam, pp 239–255

20. Casaroli G, Galbusera F, Chande R, Lindsey D, Mesiwala A, Yerby S, Brayda-Bruno M (2019) Evaluation of iliac screw, S2 alar-iliac screw and laterally placed triangular titanium implants for sacropelvic fixation in combination with posterior lumbar instrumentation: a finite element study. Eur Spine J 28(7):1724–1732

21. MacLeod AR, Pankaj P, Simpson AHR (2012) Does screw–bone interface modelling matter in finite element analyses? J Biomech 45(9):1712–1716

22. Wieding J, Souffrant R, Fritsche A et al (2012) Finite element analysis of osteosynthesis screw fixation in the bone stock: an appropriate method for automatic screw modelling. PLoS ONE 7(3):e33776

23. Noailly J, Lacroix D (2012) Finite element modelling of the spine. Biomaterials for spinal surgery. Elsevier, Amsterdam, pp 144–234e

24. Noailly J, Malandrino A, Galbusera F (2014) Computational modelling of spinal implants. In: Computational modelling of biomechanics and biotribology in the musculoskeletal system. Elsevier, Amsterdam, pp 447–484

25. Luca A, Ottardi C, Sasso M et al (2017) Instrumentation failure following pedicle subtraction osteotomy: the role of rod material, diameter, and multi-rod constructs. Eur Spine J 26(3):764–770

26. Lee S, Im Y, Kim K et al (2011) Comparison of cervical spine biomechanics after fixed-and mobile-core artificial disc replacement: a finite element analysis. Spine 36(9):700–708

27. Galbusera F, Bellini CM, Anasetti F et al (2011) Rigid and flexible spinal stabilization devices: a biomechanical comparison. Med Eng Phys 33(4):490–496

28. Rohlmann A, Burra NK, Zander T et al (2007) Comparison of the effects of bilateral posterior dynamic and rigid fixation devices on the loads in the lumbar spine: a finite element analysis. Eur Spine J 16(8):1223–1231

29. Rohlmann A, Boustani HN, Bergmann G et al (2010) Effect of a pedicle-screw-based motion preservation system on lumbar spine biomechanics: a probabilistic finite element study with subsequent sensitivity analysis. J Biomech 43(15):2963–2969

30. Tsuchiya K, Bridwell KH, Kuklo TR et al (2006) Minimum 5-year analysis of L5–S1 fusion using sacropelvic fixation (bilateral S1 and iliac screws) for spinal deformity. Spine 31(3):303–308

31. V Sabourin JL Gillick JS Harrop 2019 Instrumentation-Related Complications. In: Complications in neurosurgery. Elsevier, Amsterdam. pp 320–324

32. Weistroffer JK, Perra JH, Lonstein JE et al (2008) Complications in long fusions to the sacrum for adult scoliosis: minimum fiveyear analysis of fifty patients. Spine 33(13):1478–1483

33. Wilke HJ, Wenger K, Claes L (1998) Testing criteria for spinal implants: recommendations for the standardization of in vitro stability testing of spinal implants. Eur Spine J 7(2):148–154

34. Lindsey DP, Parrish R, Gundanna M et al (2018) Biomechanics of unilateral and bilateral sacroiliac joint stabilization. J Neurosurg Spine 28(3):326–332

35. Soriano-Baron H, Lindsey DP, Rodriguez-Martinez N et al (2015) The effect of implant placement on sacroiliac joint range of motion: posterior versus transarticular. Spine 40(9):E525–E530

36. Sutterlin CE, Field A, Ferrara LA et al (2016) Range of motion, sacral screw and rod strain in long posterior spinal constructs: a biomechanical comparison between S2 alar iliac screws with traditional fixation strategies. J Spine Surg 2(4):266–276. https: // doi.org/10.21037 /jss.2016.11.01

37. Viceconti M, Henney A, Morley-Fletcher E (2016) In silico clinical trials: how computer simulation will transform the biomedical industry. Int J Clin Trials 3(2):37–46

38. Schmidt H, Galbusera F, Rohlmann A et al (2012) Effect of multilevel lumbar disc arthroplasty on spine kinematics and facet joint loads in flexion and extension: a finite element analysis. Eur Spine J 21(Suppl 5):S663–S674. https ://doi.org/10.1007/s0058 6-010-1382-1

39. Dreischarf M, Rohlmann A, Bergmann G et al (2011) Optimised loads for the simulation of axial rotation in the lumbar spine. J Biomech 44(12):2323–2327. https ://doi.org/10.1016/j.jbiom ech.2011.05.040

40. Rohlmann A, Zander T, Rao M et al (2009) Applying a follower load delivers realistic results for simulating standing. J Biomech 42(10):1520–1526. https ://doi.org/10.1016/j.jbiom ech.2009.03.048

41. Rohlmann A, Zander T, Rao M et al (2009) Realistic loading conditions for upper body bending. J Biomech 42(7):884–890. https ://doi.org/10.1016/j.jbiom ech.2009.01.017

42. Chevalier Y, Matsuura M, Krüger S et al (2018) Micro-CT and micro-FE analysis of pedicle screw fixation under different loading conditions. J Biomech 70:204–211